Young's modulus characterization of low-*k* films of nanoporous Black Diamond™ by surface acoustic waves*

Shan Xingmeng(单兴锰), Xiao Xia(肖夏)†, and Liu Yaliang(刘亚亮)

(School of Electronic and Information Engineering, Tianjin University, Tianjin 300072, China)

Abstract: The laser-generated surface acoustic wave (SAW) technique is an accurate, fast and nondestructive solution to determine the mechanical properties of ultra thin films. SAWs are dispersive during the wave propagation on the layered structure. The Young's moduli of thin films can be obtained by matching the experimentally and theoretically calculated dispersive SAW curves. A short ultraviolet laser pulse is employed to generate the broad spectral range of the dispersive SAWs. The frequency range of dispersive SAWs in this study reaches 180 MHz, which is adequate for the SAW technique applied for the investigated samples. In this work, the Young's moduli of a series of nanoporous Black Diamond™ low dielectric constant (low-*k*) films deposited on a Si (100) substrate are characterized successfully by the SAW technique.

Key words: ULSI interconnect; SAWs; Young's modulus; Black Diamond™; nanoporous low-*k* film
DOI: 10.1088/1674-4926/31/8/082002 **PACC:** 8170C; 4885G; 6825

1. Introduction

One of the most significant challenges for ultralarge-scale integration (ULSI) interconnect systems is to introduce new materials to meet the requirements for wire conductivity and dielectric permittivity. Compared with the conventional Al/SiO_2 technology, integration of Cu and low-*k* dielectrics has incrementally improved the situation by reducing both resistivity and capacitance between wires[1, 2]. Black Diamond™ is a type of promising low-*k* material and has been integrated with copper interconnect. To acquire lower *k* values, nanopores are introduced into the dielectrics. However, the mechanical performance of films with nanopores is very poor owing to the agglomeration and coalescence of the pores during the process of adding porogen to precursor solutions. The poor mechanical characters may lead to serious reliability problems and limit the chemical mechanical polishing (CMP) process of ULSI[3, 4]. Therefore, it is very significant to check the mechanical properties of nanoporous Black Diamond™ low-*k* film in evaluating the overall performance of the developed material.

Young's modulus is one of the most important mechanical properties. Several techniques such as nanoindentation, surface Brillouin light scattering, and surface acoustic wave have been developed to determine Young's modulus. Nanoindentation is a traditional method for Young's modulus detection. In this technique, a diamond indenter is pressed into the sample with a certain load and then is uplifted by releasing the load. The Young's modulus of the indented film can be extracted by analyzing the load-displacement correlation[5, 6]. However, the nanoindentation results are uncertain for viscoelastic solids and very thin films (where the thickness of the film is smaller than 1 μm), particularly for a soft film on a stiff substrate structure[7]. When testing with a Berkovich tip, this effect typically begins to appear at depths measuring 10% of the overall film thickness and is aggravated as the depth increases[8]. The reasons for the inaccuracy may be due to substrate stiffening, film viscoelasticity, tip-film interaction, the choice of indenter shape, the indentation size, the depth, the load, and so on[9−12]. Many measures such as the "effectively shaped indenter concept" and "a sharper and more acute cube corner tip" as well as data analyses and processing techniques have been proposed to improve the feasibility of the nanoindentation on measuring the mechanical properties of ultra thin and soft films[7, 13−16]. However, even very shallow indents (< 10% of the film thickness) are compromised by substrate effects and the post data processes are very complicated[14−16]. Besides, the nanoindentation method is destructive and not suitable for online tests.

Surface Brillouin light scattering measures the surface wave dispersion, which is based on the inelastic interaction between laser photons and acoustic phonons of the sample[1, 7]. It is nondestructive and has a wide wave frequency range, but it is a very time consuming method and sensitive to the environment noise. Instead, the surface acoustic wave (SAW) method is an attractive method especially for ultra thin low-*k* films[18−20]. SAWs are generated by thermal–elastic interaction during the energy adsorption of the short impulse laser. SAWs are dispersive during propagation on the layered structure, which takes not only the layer but also the substrate material properties into account from the principle. Therefore, the SAW technique can eliminate the influence of the hard substrate, which is inevitable in the nanoindentation technique, and it is much faster than the surface Brillouin light scattering approach.

In this work, the theoretical study and experimental details of the laser-generated SAW technique are presented. Signal processing with a finite impulse response (FIR) filter is applied to decrease the noise of the detected SAW signals. Young's

* Project supported by the National Natural Science Foundation of China (No. 60876072) and the New Century Excellent Talents in University, China (No. NCET-08-0389).
† Corresponding author. Email: xiaxiao@tju.edu.cn
Received 22 February 2010, revised manuscript received 14 April 2010

moduli are obtained for nanoporous Black Diamond^{TM} low-k films by matching the experimental and theoretical dispersion curves. The factors which influence the SAW determination results are discussed in detail.

2. Theoretical study and experiment details

2.1. Theoretical study of SAWs

When the energy of a focused laser pulse with pulse width in the nanosecond or picosecond range is absorbed on the surface of a sample, a fast thermal expansion on the sample occurs and consequently leads to the generation of surface acoustic waves. Effective SAW generation happens when the laser pulse width is shorter than the acoustic transit time. The energy of the laser is carefully chosen to create the adequate signal amplitude of SAWs and to avoid the ablation of sample surface, simultaneously[21, 22]. During the propagation of surface acoustic waves, most of their energy is closely limited to the surface and the depths of elastic displacements and stresses caused by SAWs are approximately one wavelength. SAWs are dispersive when the waves propagate on a layered structure. High frequency SAWs are mainly affected by the thin film, while the low frequency SAW parts carry more information on the substrate. The dispersion of SAWs can be described as

$$v_{\mathrm{SAW}} = F\left(f, (E, \rho, \sigma, h)_{\mathrm{layer}}, (c_{ijkl}, \rho_{\mathrm{s}})_{\mathrm{substrate}}\right), \quad (1)$$

where v_{SAW} is the frequency dependent velocity, f is the frequency of the SAWs, and E, ρ, σ and h are the Young's modulus, density, Poisson's ratio and thickness of the layer film, respectively. Parameters c_{ijkl} and ρ_{s} are the elastic constants and density of the substrate. The values of c_{11}, c_{12}, c_{44} and ρ of Si substrate are 165.7, 63.9, 79.6 GPa, and 2.33 g/cm^3, respectively[17]. When SAWs propagate along the [110] direction on the silicon (100) plane, the dispersion degree of the SAWs is little affected by the Poisson's ratio σ of the layer film but mainly depends on its Young's modulus[23]. Thus, theoretical dispersion curves with different Young's moduli (E) can be calculated according to the wave motion theory. In the experimental system, which will be discussed in Section 2.2, SAWs are detected at two positions to obtain the experimental dispersion curve, which can be calculated by

$$v(f) = \frac{2\pi(d_2 - d_1)}{\Phi_2(f) - \Phi_1(f)}, \quad (2)$$

where $v(f)$ is the phase velocity, f is the frequency, d_i is the distance between the piezoelectric transducer and the position of the laser source, and $\Phi_i(f)$ is the phase angle of SAWs. The Young's modulus of the detected layer film can be determined by fitting the experimental dispersion curve with the theoretically calculated dispersion curves.

2.2. Experimental details

The experimental system schematic diagram for SAW detection is shown in Fig. 1. The surface acoustic waves are generated by a nitrogen laser with a wavelength of 337.1 nm and a pulse width of 800 ps. The laser is focused into a line light source by a cylindrical lens and irradiates the detected sample. The energy irradiated on the surface of the sample is 109 μJ.

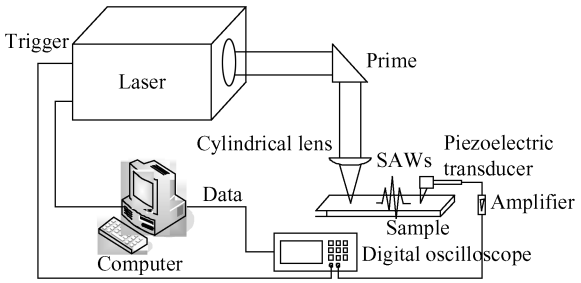

Fig. 1. Schematic diagram of the SAW signals detection system.

Table 1. Film thickness of the porous Black Diamond^{TM} low-k samples.

Sample	1	2	3
Thickness (nm)	197.3	304.5	510.2

Three nanoporous Black Diamond^{TM} low-k films with different thicknesses are detected in this measurement. The dielectric constant, porosity, and density of the low-k films are 2.4, 23%, and 1.1 g/cm^3, respectively. The thicknesses are listed in Table 1. A piezoelectric transducer is applied to transfer the mechanical vibrations of the SAWs into electrical signals. It is made up of a wedge tip with a very thin polyvinilydene fluoride (PVDF) foil pressed on. The thickness of the PVDF foil is 9 μm to ensure a broadband signal conversion. The minimum response time of the PVDF foil is 4 ns[21], indicating that the bandwidth of converted signals could be reached at a frequency of 250 MHz. After signal amplification by an ultra low noise amplifier, signals are collected through a digital oscilloscope. The experimental dispersion curve could be obtained from the recorded signals through the calculation based on Eq. (2).

There are two key points for the experimental system: (1) the electromagnetic shielding and (2) the alignment of line laser source and the wedge edge of the piezoelectric transducer. As the detected SAW signals are very weak, the electromagnetic interference is the main noise source to disturb the effective SAW signal. Therefore, a copper net is used here for shielding the external electromagnetic noise. The piezoelectric transducer and sample are surrounded by the copper net, and an open hole is designed at the top of the copper net to let the laser beam pass through and irradiate the sample via the designed optical path. The signal-to-noise ratio (SNR) of SAW signals could be improved up to 50 : 1 by the copper net electromagnetic shielding.

In this experiment, sagittal SAW waves, which are shown in Fig. 2(a), are generated by the line laser source. This is easier for theoretical calculation and experimental measurement than the case in which the SAWs are generated by a laser spot source as shown in Fig. 2(b). To ensure that the experimental detection matches the theoretical computation for the case of sagittal waves, the line laser source and the wedge edge of the piezoelectric transducer must be parallel. As the SAW signals should be detected at two positions according to Eq. (2), the piezoelectric detector is fixed while the prime and cylindrical lens are moved together to shift the laser line in order to generate SAWs at different positions. In this experiment, the lengths of the line laser source and the transducer edge are 12 mm and

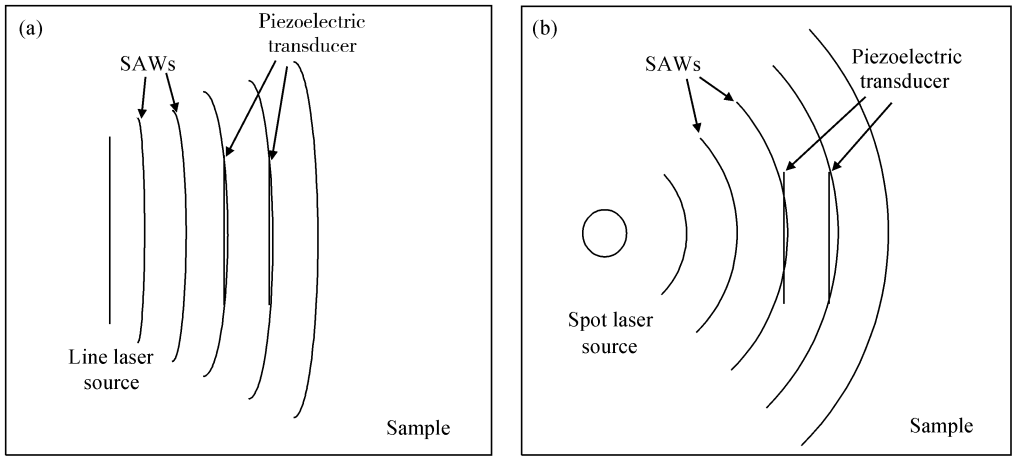

Fig. 2. SAWs generated by line and spot laser sources. (a) SAWs generated by a line laser source. (b) SAWs generated by a spot source.

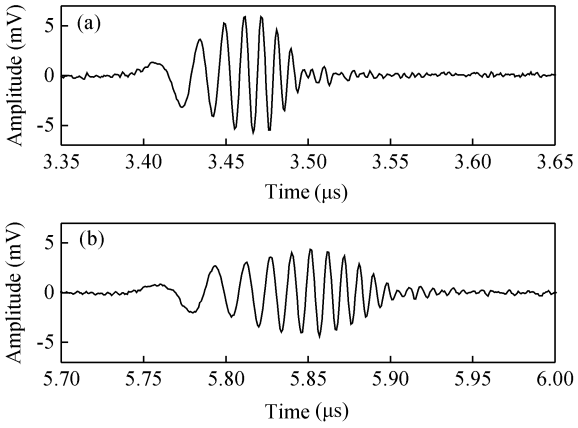

Fig. 3. SAW signals of sample 3 detected at (a) position 1 and (b) position 2.

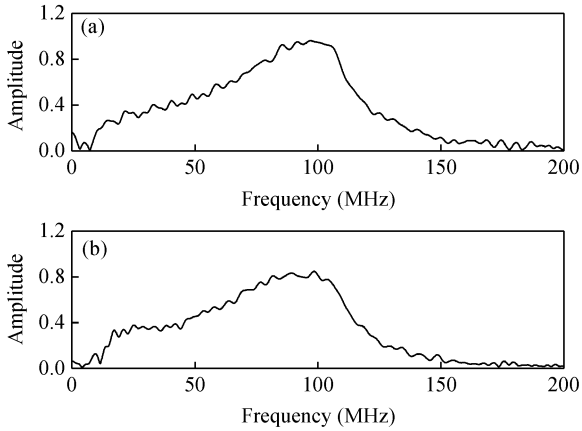

Fig. 4. Amplitude frequency spectrum of SAW signals at (a) position 1 and (b) position 2.

10 mm, respectively. The distance between two detection positions is 12 mm. SAW signals for sample 3 derived from the experimental system are shown in Fig. 3. There is an apparent delay between the two signals, because they are collected at different positions. The time difference between these two waves is about 2.35 μs, and the velocity of SAWs propagating along the [110] direction on the Si (100) plane is 5082 m/s, so the distance between the two detection positions can be estimated approximately by 5082 m/s $\times$ 2.35 μs = 11.94 mm, which agrees very well with the distance of 12 mm designed in our experiment. This estimation confirms the correctness of the experimental signal detection.

3. Result and discussion

3.1. Signal processing

Although the experimental system is carefully shielded by the copper net, noise still exists and affects the fitting procedure for determining the Young's modulus of the film. In this work, a band pass FIR filter loaded with a Kaiser window is employed to minimize the noise. The designed FIR band pass filter keeps the SAW signals of interest within a certain frequency range and filters out the undesired noise. The bandwidth of effective SAW signals in this study is 30 to 180 MHz, so the frequency range of the band pass FIR filter is designed from 20 to 200 MHz, which is a little wider than that of the effective signals. The "Gibbs effect" of the FIR filter can be decreased by loading the Kaiser window. After this filtering process, fast Fourier transform (FFT) is applied to process the signals to obtain the phase frequency character of the SAWs. The phase character is required to extract the experimental SAW dispersion curve according to Eq. (2). Figures 4 and 5 show the normalized amplitude and phase frequency spectrum of SAW signals for sample 3, respectively.

3.2. Experimental result

After the signal processing, the experimental dispersion curves could be calculated by Eq. (2). The Young's modulus (E) of the thin film could be obtained by matching the experimental and theoretical dispersion curves. This procedure is realized by identifying the least square variance between the experimental and theoretical dispersion curves. By calculating the variances of the above curves, the E value of the theoretical dispersion curve with the least variance is determined as the Young's modulus of the thin film. The experimental and theoretical dispersion curves are shown in Fig. 6, where solid

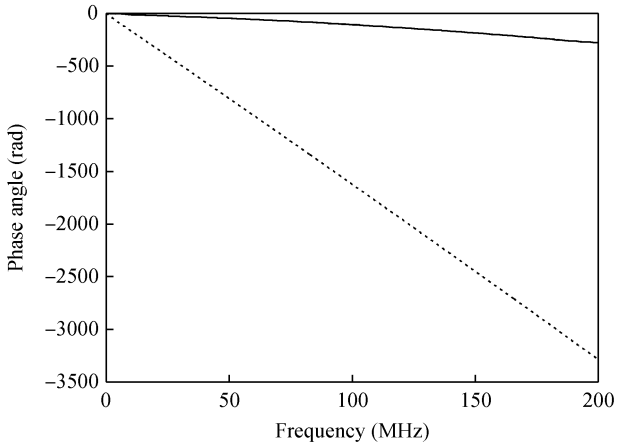

Fig. 5. Phase frequency spectrum of SAW signals. The solid line is measured at position 1 and the dotted line is measured at position 2.

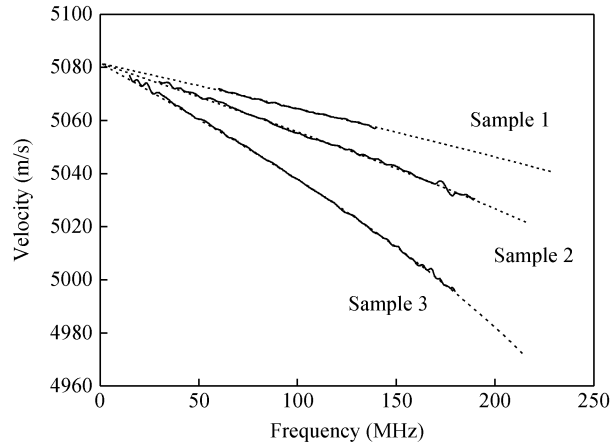

Fig. 6. Experimental and theoretical dispersion curves of SAWs. Solid lines and dotted lines are the experimental and theoretical dispersion curves, respectively.

Table 2. Young's modulus of the porous Black Diamond^{TM} low-k samples.

Sample	1	2	3
Yong's modulus (GPa)	1.12	1.34	1.83

lines and dotted lines are experimental and theoretical dispersion curves, respectively. The determined Young's moduli for the three detected Black Diamond^{TM} low-k thin films are listed in Table 2.

3.3. Analysis and discussion

The obvious dispersion of SAWs is shown in Fig. 6. The dispersion is due to the velocity difference of the wave propagating along the surface of the low-k film and the silicon substrate. The velocity of the surface wave propagating along the [110] direction of Si (100) is 5082 m/s, which is faster than that in the soft low-k film. High frequency parts of SAWs are mainly influenced by the layered structure, while the low frequency waves mainly depend on the silicon substrate. This is the reason that velocities in the dispersion curve of SAWs descend with increasing frequency. This phenomenon is also indicated from the original SAW waveforms in Fig. 3, in which the earlier-arriving SAW signals are relatively incompact compared to later-arriving waves.

As shown in Fig. 6, the curvature of the dispersion curve is smaller for the thinner film, which indicates that the phase velocities change little with the change of E value. Then the accuracy of the determined Young's modulus for the low-k films is very dependent on the experimental detection. To improve the determination precision, SAW signals are detected at each position sixteen times, averaged for dispersion curve calculation. Moreover, four dispersion curves are calculated for each sample, and the averaged curve is adopted in the fitting process to extract the final result of the film's Young's modulus. In our current experimental system, the repetition and stability is very good with a result deviation of only 0.1 GPa.

However, extra measures are desired to improve this promising technique. The extension of the SAW bandwidth to higher frequencies is very helpful for the fitting process. The piezoelectric transducer needs to be improved to enlarge the bandwidth of SAWs[18, 24]. The determining results of E values might be affected by the surface roughness and the interface adhesion between the film and substrate[19]. Further investigation will be carried in our future research.

4. Conclusion

Young's modulus detection for fragile nanoporous Black Diamond^{TM} low-k films by surface acoustic waves is presented in this paper. SAW signals generated by a short laser pulse are detected by the piezoelectric transducer after propagating for a certain distance. The influences of the electromagnetic shielding, the alignment of the laser line source and the wedge edge of the piezoelectric transducer on the measurement are discussed. An FIR filter loaded with a Kaiser window is applied to the original SAW signals to reduce the noise. Smooth experimental dispersion curves with a spectral range up to 180 MHz are achieved. The least square variance of the experimental and theoretical dispersion curves is calculated in the fitting process to determine the Young's modulus of the film. The Young's moduli of nanoporous Black Diamond^{TM} low-k samples with different thicknesses of 197.3, 304.5 and 510.2 nm have been investigated. The determined Young's moduli for these three low-k films are 1.12, 1.34 and 1.83 GPa, respectively. Furthermore, the influencing factors on the accuracy of the SAW technique are discussed.

Acknowledgment

The authors would like to thank the Chartered Semiconductor Manufacturing Ltd for sample preparation.

References

[1] International technology roadmap for semiconductors. Interconnect, Semiconductor Industry Association, 2007
[2] Maex K, Baklanov M R, Shamiryan D, et al. Low dielectric constant materials for microelectronics. J Appl Phys, 2003, 93: 8793
[3] Li B, Sullivan T D, Lee T C, et al. Reliability challenges for copper interconnects. Microelectron Reliab, 2004, 44: 365
[4] Schulze K, Schulz S E, Frühauf S, et al. Improvement of mechanical integrity of ultra low k dielectric stack and CMP compatibility. Microelectron Eng, 2004, 76: 38

[5] Cherault N, Carlotti G, Casanova N, et al. Mechanical characterization of low-*k* and barrier dielectric thin films. Microelectron Eng, 2005, 82: 368
[6] Nay R J, Warren O L, Yang D, et al. Mechanical characterization of low-*k* dielectric materials using nanoindentation. Microelectron Eng, 2004, 75: 10
[7] Richter F, Herrmann M, Molnar F, et al. Substrate influence in Young's modulus determination of thin films by indentation methods: cubic boron nitride as an example. Surf Coat Technol, 2006, 201: 3577
[8] Fischer-Cripps A. Nanoindentations. New York: Springer-Verlag, 2002
[9] Murray C, Flannery C, Streiter I, et al. Comparison of techniques to characterise the density, porosity and elastic modulus of porous low-*k* SiO_2 xerogel films. Microelectron Eng, 2002, 60: 133
[10] Herbert E G, Oliver W C, Pharr G M. Nanoindentation and the dynamic characterization of viscoelastic solids. J Phys D: Appl Phys, 2008, 41: 074021
[11] Herbert E G, Oliver W C, Pharr G M. On the measurement of yield strength by spherical indentation. Philosophical Magazine, 2006, 86: 5521
[12] Flannery C M, Wittkowski T, Jung K, et al. Critical properties of nanoporous low dielectric constant films revealed by Brillouin light scattering and surface acoustic wave spectroscopy. Appl Phys Lett, 2002, 80: 4594
[13] Herrmann M, Richter F. On the usage of the effectively shaped indenter concept for analysis of yield strength. J Mater Res, 2009, 24: 1258
[14] Herrmann A, Schwarzer N, Richter F, et al. Determination of Young's modulus and yield stress of porous low-*k* materials by nanoindentation. Surf Coat Technol, 2006, 201: 4305
[15] Herrmann M, Richter F. Determination of Young's modulus and yield strength of porous low-*k* dielectric films by nanoindentation under complete consideration of the substrate influence. Int J Surf Sci Eng, 2009, 3: 64
[16] Nay R J, Warren O L, Yang D, et al. Mechanical characterization of low-*k* dielectric materials using nanoindentation. Microelectron Eng, 2004, 75: 103
[17] Lefeuvre O, Pang W, Zinin P, et al. Determination of the elastic properties of a barrier film on aluminium by Brillouin spectroscopy. Thin Solid Films, 1999, 350: 53
[18] Schneider D, Fruhauf S, Schulz S E, et al. The current limits of the laser-acoustic test method to characterize low-*k* films. Microelectron Eng, 2005, 82: 398
[19] Xiao Xia, Shan Xingmeng, Liu Yaliang. Evaluating of adhesion property of ULSI interconnect films by the surface acoustic waves. Chin Phys Lett, 2010, 27: 018502
[20] Xiao Xia, You Xueyi. Numerical study on surface acoustic wave method for determining Young's modulus of low-*k* films involved in multi-layered structures. Appl Surf Sci, 2006, 253: 2958
[21] Paltauf G, Schmidt-Kloiber H. Pulsed optoacoustic characterization of layered media. J Appl Phys, 2000, 88: 1624
[22] Gospodyn J P, Sardarli A, Brodnikovski A M, et al. Ablatiive generation of surface acoustic waves in aluminum using ultraviolet laser pulses. J Appl Phys, 2002, 92: 564
[23] Takimura T, Hata N, Takada S, et al. Determination of mechanical properties of porous silica low-*k* films on Si substrates using orientation dependence of surface acoustic wave. Jpn J Appl Phys, 2008, 47: 5400
[24] Xiao X, Hata N, Yamada K, et al. Mechanical property determination of thin porous low-*k* films by twin-transducer laser generated surface acoustic waves. Jpn J Appl Phys, 2004, 43: 508